Turkish Journal of Physics

Volume 42 | Number 3 Article 12

1-1-2018

Tailoring the magnetic anisotropy of cobalt-gold thin films

CENGİZ OKAY

PERİHAN AKSU

CANER DEGER

FİKRET YILDIZ

TÜBİTAK

Turkish Journal of Physics

http://journals.tubitak.gov.tr/physics/

Research Article

Turk J Phys
(2018) 42: 335 – 341

doi:10.3906/fiz-1802-33

Tailoring the magnetic anisotropy of cobalt-gold thin films

Cengiz OKAY[1], Perihan AKSU[2], Caner DEĞER[1,*], Fikret YILDIZ[3]
[1]Department of Physics, Faculty of Science, Marmara University, Göztepe, İstanbul, Turkey
[2]Institute of Nanotechnology, Gebze Technical University, Gebze, Kocaeli, Turkey
[3]Department of Physics, Faculty of Science, Gebze Technical University, Gebze, Kocaeli, Turkey

Received: 22.02.2018 • **Accepted/Published Online:** 16.05.2018 • **Final Version:** 01.06.2018

Abstract: Magnetic cobalt-gold thin films ($Co_x Au_{(1-x)}$) are grown on silicon (100) surfaces by using a sputter deposition technique. Magnetic anisotropy of the films is investigated by ferromagnetic resonance (FMR). Magnetic properties are explored by micromagnetic simulations based on the metropolis algorithm. Effective magnetic anisotropy is gradually increased with Co concentration. In-plane axial anisotropy exists for all samples and it is enhanced with a Co concentration of ∼40%, corresponding optimal cluster size, and intercluster separation. Segregation and coalescence of Co clusters caused by different Co concentrations strongly affect magnetic properties of the thin films. Therefore, the study revealed that magnetic behavior of $Co_x Au_{(1-x)}$ thin films can be tuned by changing Co concentration.

Key words: Magnetosputtering, magnetic thin films, ferromagnetic resonance, magnetic anisotropy

1. Introduction

In past decades, spin-based electronics (spintronics) attracted the attention of many researchers. Metallic spintronic devices [1], originating from the discovery of giant magnetoresistance (GMR) [1,2], such as hard disk read heads and magnetic random access memory, are among the most advanced technologies. A few studies explained the behavior of spins in metal [3] and magnetoresistive devices [3–5] including GMR and tunneling magnetoresistance [6]. Spintronic devices (such as magnetoelectronic devices, spin valves, etc.) operate very fast, have high data storage density, and consume less electrical power when compared to conventional devices [7]. The combination of magnetic materials (cobalt, iron, nickel, etc.) with noble metals such as gold, silver, or platinum offers a suitable platform for technological applications such as magnetoplasmonic sensors and novel fields of scientific studies [8–13]. Co/Au interfaces have particularly attracted attention and are extensively explored because of their remarkable magnetic properties. The microstructure and ferromagnetic resonance (FMR) properties of Co/Au multilayers were investigated by Rizal [14] and Kehagias et al. [15]. It was revealed that sputter-grown Co/Au MLs, with (111) texture, exhibit low-field GMR due to low magnetocrystalline anisotropy in Co layers. Moreover, Hrubovčák et al. studied magnetic properties and relaxation processes in Co/Au bimetallic nanoparticles [16].

In order to discover less stringent material designs, the possibility of using nanocomposite Co-Au thin films is considered. In the study performed by Yang et al. [9], Co-Au composite thin films with various Co:Au concentrations from 5:95 to 60:40 with various grown temperatures from room temperature to 600 °C but with

*Correspondence: caner.deger@marmara.edu.tr

fixed total thickness were prepared using magnetron sputtering codeposition. Strong enhancement of the magnetooptical activity was observed when surface plasmon polaritons were excited in the nanocomposite films. In another study on Co-Au cosputtered thin films, it was revealed that the local magnetization contrast affects the nonlinear magnetooptical properties as well as the magnetotransport properties in magnetic metal/nonmagnetic metal multilayers; thus, nanocomposite films showcase another path to investigate possible correlations between these distinct properties, which may prove useful for sensing applications [17].

Nevertheless, the crystal structure and magnetic properties of Co-Au films have not been fully studied and there are a number of open questions such as the effect of Co:Au content ratio on crystal structures and magnetic behavior. In this study, magnetic properties of Co-Au thin films with different cobalt concentrations ($\mathrm{Co}_x\mathrm{Au}_{(1-x)}$, where x = 0.25–0.60) were investigated both theoretically and experimentally. Magnetic measurements were performed by ferromagnetic resonance technique. A theoretical model and in-house codes based on the Markov chain Monte Carlo method were developed to analyze the FMR spectra.

2. Experimental procedures

Cobalt-gold [$\mathrm{Co}_x\mathrm{Au}_{(1-x)}$] magnetic thin film alloys have been fabricated on Si (100) substrate by using a magnetosputter technique. Si (100) substrates were chemically cleaned before introducing them into the chamber and they were annealed at 500 °C in vacuum for 1 h. Base pressure of the chamber is $\sim 2 \times 10^{-9}$ mbar and during deposition it is $\sim 1 \times 10^{-3}$ mbar. During growth of the $\mathrm{Co}_x\mathrm{Au}_{1-x}$ thin films, the substrate was at room temperature. The crystal structure of a sample was investigated using a Rigaku 2000 DMAX diffractometer. X-band FMR measurements were performed with a JEOL series (JES FA 300) ESR spectrometer. The FMR spectra were recorded by varying orientations of the film surface with respect to the applied DC magnetic field (H).

3. Model and simulations

Even if ferromagnetic resonance measurements provide immense information about magnetic properties of matter, further quantitative analysis of the sample such as determining effective magnetization and anisotropy constants is only possible with micromagnetic simulations [8,13]. The energy Hamiltonian of the system we modeled to analyze our sample set is described by the following equation:

$$\mathcal{H} = \left\{ \begin{array}{l} -MH\left[\cos(\theta_H)\cos(\theta) + \sin(\theta_H)\sin(\theta)\cos(\varphi_H - \varphi)\right] \\ +K_{eff}\cos^2(\theta) \\ -K_{ax}\sin^2(\theta)\cos^2(\varphi) \end{array} \right\} \quad (1)$$

Here, (θ, θ_H) and (φ, φ_H) are respectively the polar and azimuth angles for magnetization vector **M** and external DC field vector **H** with respect to the film plane. The first term of the Hamiltonian is the Zeeman energy of the film in external DC field. The second term represents the magnetostatic energy due to the demagnetizing field. The last term represents the presumed in-plane-induced uniaxial anisotropy energy due to film preparation conditions. M, K_{eff}, and K_{ax} are the saturation magnetization, effective anisotropy energy density, and the axial anisotropy constant, respectively.

The external magnetic field is scanned from 0 to 1000 mT to determine the field corresponding to the maximum value of χ_2, which called the resonance field (H_{res}). Dynamic susceptibility spectrum χ_2 is calculated

using the following equation [18–20]:

$$\chi_2 = \frac{4\pi M_0 \left(Dk^2 + \frac{1}{M_0}\frac{\partial^2 E}{\partial \theta^2} \right) \frac{2\omega}{\gamma^2 T_2}}{\left[\left(\frac{\omega_0}{\gamma} \right)^2 - \left(\frac{\omega}{\gamma} \right)^2 \right]^2 - \frac{4\omega^2}{\gamma^4 T_2^2}} \tag{2}$$

Here, ω_0 is the precessional frequency of the system, the Larmor frequency, which is calculated by the following equation [21]:

$$\left[\frac{\omega_0}{\gamma} \right]^2 = \left[Dk^2 + \frac{1}{M_0}\frac{\partial^2 E_{Total}}{\partial \theta^2} \right] \left[Dk^2 + \frac{1}{M_0 \sin^2\theta}\frac{\partial^2 E_{Total}}{\partial \varphi^2} \right] - \left(\frac{1}{M_0 \sin^2\theta}\frac{\partial^2 E_{Total}}{\partial \theta \ \partial \varphi} \right)^2 \tag{3}$$

As the external magnetic field increases, the Larmor frequency gets closer to the resonance frequency of microwave radiation ω and then dynamic susceptibility X_2 starts to increase because of the decreasing ω – ω_0 difference. At $\omega = \omega_0$, the corresponding external magnetic field is marked as the resonance field for both parallel and perpendicular geometry [8,22]. All calculations are performed at room temperature to fit with the experimental data. M, ω/γ, K_{eff}, and K_{ax} are obtained by the simulations for all five samples. Here, the Markov chain Monte Carlo step number is 2×10^6.

4. Results and discussion

Although extensive work has been carried out regarding the magnetotransport and magnetooptical properties of Au-Co films [17,23,24], the FMR study of Co-Au thin films has not been investigated to the best of our knowledge. Hence, room temperature ferromagnetism in $Co_x Au_{(1-x)}$ thin film alloys where x = 0.25, 0.33, 0.40, 0.48, and 0.61 on silicon (100) substrate has been observed by FMR. We performed the measurements for two different geometries as shown in Figure 1. One is parallel geometry where the DC magnetic field remains parallel to the film plane and the sample rotates around the film normal. The other is perpendicular geometry where the DC magnetic field is aligned perpendicular to the sample surface. FMR spectra of the samples are represented in Figure 1. The easy axis of magnetization is in-plane for all concentrations. The signal becomes stronger with increasing x. Angular dependency of the peak can be seen in Figure 2.

A special computer program [8,22] introduced in Section 3 part has been used to extract the parameters of saturation magnetization (M_S), effective anisotropy energy density (K_{eff}), and axial anisotropy constant (K_{ax}). Results of the modeling (best fit line) are also presented in Figure 2 by solid lines and obtained parameters are given in the Table. Here, ω/γ is 0.3275 T for all samples.

Axial anisotropy constant K_{ax} is gradually increasing from 0.09×10^4 to 2.30×10^4 J/m^3 excluding x = 0.40, as seen in the Table. Interestingly, the maximum K_{ax} value appears for the sample that includes 40% Co. This percentage corresponds to optimal cluster size (typical grain radius of 1.4 nm) [24] and intercluster separation for the Co-Au system [25,26]. The interface between Co clusters and the Au matrix is maximum in this sample. This maximal area of interface may induce addition axial anisotropy. A Co concentration below 40% causes a small amount of magnetic clusters, leading to a decrease in K_{ax}. Briefly, increase in Co concentration leads to increased axial anisotropy until an optimal value is reached, beyond which it decreases again since

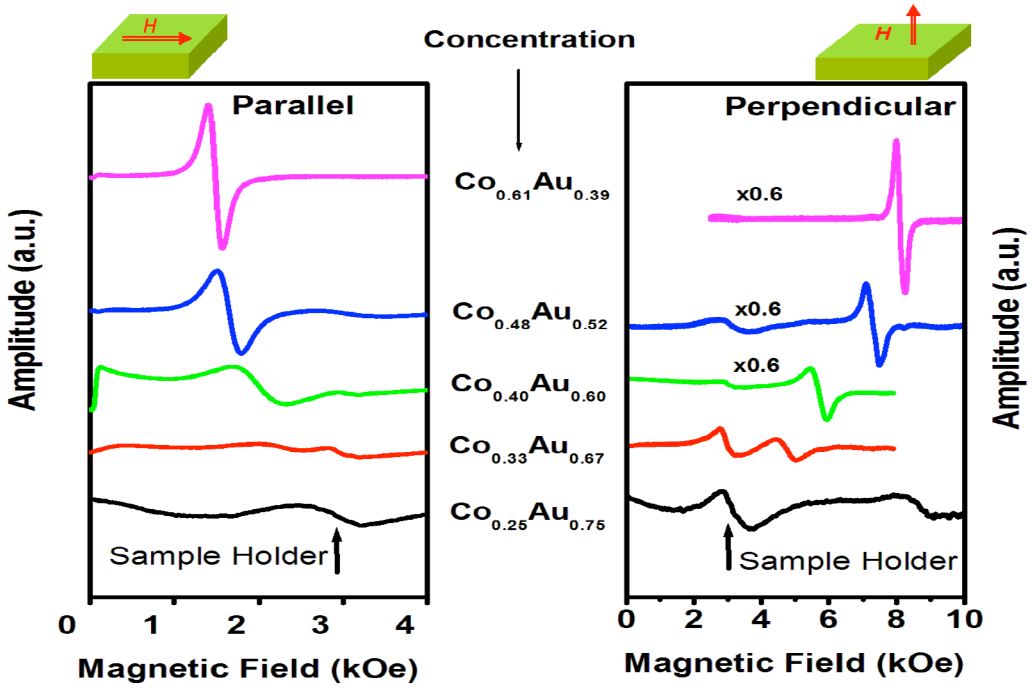

Figure 1. FMR spectra of samples for different cobalt-gold concentrations on Si (100) substrate, measured at parallel and perpendicular orientations of film plane to magnetic field.

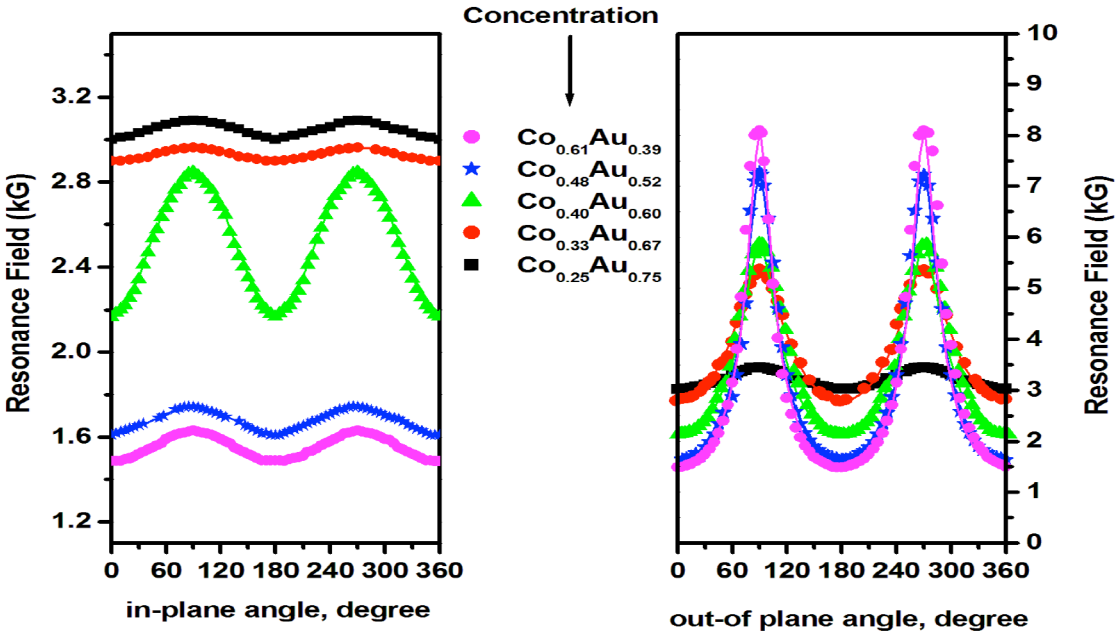

Figure 2. Angular dependence of magnetic resonance fields with different cobalt-gold concentrations on Si (100) substrate. The symbols present the experimental values; the solid lines show the best fits.

the magnetic clusters have now coalesced and percolated [17,27,28]. We also performed XRD measurements to support the Co cluster formation in $Co_{0.4}Au_{0.6}$ thin films, which can be seen in Figure 3.

Table. Magnetic characteristics of thin film alloys with different cobalt-gold concentrations.

Co/Au concentration	M (kA/m)	K_{eff} (10^5 J/m^3)	K_{ax} (10^4 J/m^3)
0.25/0.75	3.183	–0.01	0.09
0.33/0.67	20.690	–0.35	0.72
0.40/0.60	25.464	–1.75	6.79
0.48/0.52	32.626	–2.55	2.01
0.61/0.39	35.014	–2.95	2.30

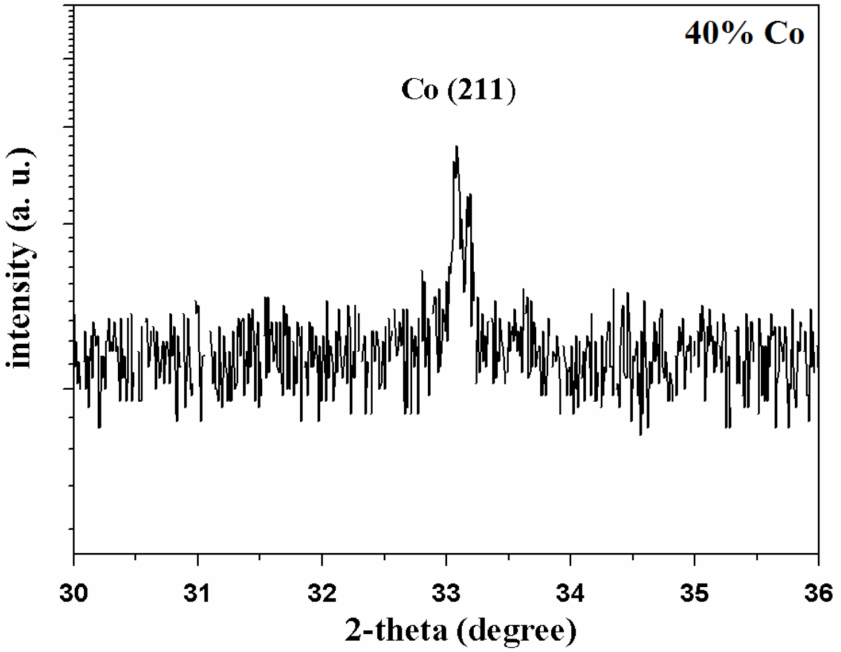

Figure 3. X-ray diffraction pattern of the $Co_{0.4}Au_{0.6}$ thin film alloys on silicon (100) substrate.

In Figure 3, a peak around $2\theta = 33.2^\circ$ is attributed to reflections from the (211) plane of hexagonal-close-packed (hcp) Co clusters embedded in the amorphous Co-Au thin film alloys [29]. This means that, for lower concentrations of Co, Co ions in the alloy give preference to constructing Co (211) clusters instead of amorphous structures.

In the perpendicular geometry, the resonance field of the samples is strictly dependent upon Co concentration. The discussion about effects of Co concentration on cluster growth for the parallel geometry is also valid for perpendicular geometry, excluding the exotic behavior of x = 0.40. In this case, an increase in magnetic anisotropy is directly proportional to Co concentration without any exceptions. In short, magnetic properties of the Co-Au system resemble those of Co thin film with increasing x. In the presence of coalesced Co clusters, additional interactions that could affect magnetic properties such as the intercluster or interface interactions are negligible.

5. Conclusion

The magnetic properties of Co-Au thin film alloys with various cobalt/gold concentration in silicon (100) substrate are investigated by FMR measurements. We find that lower Co concentrations in $Co_xAu_{(1-x)}$ construct

segregate (211) magnetic nanoclusters. Changing composition of the $Co_x Au_{(1-x)}$ thin film affects not only the microstructure of the thin film but also the absorption of microwaves in FMR. Increase in Co concentration leads to enhanced axial anisotropy until a certain value (x = 0.40 results in optimal cluster size and separation), beyond which it decreases again since the magnetic clusters have coalesced and percolated. Also, effective magnetic anisotropy (K_{eff}) and saturation magnetization (M) are strictly dependent upon Co concentration. Our findings can be useful for technological applications such as magnetooptic and magnetotransport based sensors.

Acknowledgment

This work was supported by the Research Fund of Marmara University, Project Number FEN-A-110316-0097.

References

[1] Ziese, M.; Thornton, M. J. *Spin Electronics*; Springer: New York, NY, USA, 2001.

[2] Baibich, M. N.; Broto, J. M.; Fert, A.; Van Dau, F. N.; Petroff, F.; Etienne, P.; Creuzet, G.; Friederich, A; Chazelas, J. *Phys. Rev. Lett.* **1988**, *61*, 2472-2475.

[3] Binasch, G.; Grünberg, P.; Saurenbach, F.; Zinn, W. *Phys. Rev. B* **1989**, *39*, 4828-4830.

[4] Barnaś, J.; Fuss, A.; Camley, R. E.; Grünberg, P.; Zinn, W. *Phys. Rev. B* **1990**, *42*, 8110-8120.

[5] Camley, R. E.; Barnaś, J. *Phys. Rev. Lett.* **1989**, *63*, 664-667.

[6] Moodera, J. S.; Kinder, L. R.; Wong, T. M.; Meservey, R. *Phys. Rev. Lett.* **1995**, *74*, 3273-3276.

[7] Awschalom, D. D.; Flatté, M. E. *Nat. Phys.* **2007**, *3*, 153-159.

[8] Kalaycı, T.; Deger, C.; Akbulut, S.; Yildiz, F. *J. Magn. Magn. Mater.* **2017**, *436*, 11-16.

[9] Yang, K.; Clavero, C.; Skuza, J. R.; Varela, M.; Lukaszew, R. A. *J. Appl. Phys.* **2010**, *107*, 103924.

[10] Soares, M. M.; De Santis, M.; Tolentino, H. C.; Ramos, A. Y.; El Jawad, M.; Gauthier, Y.; Yildiz, F.; Przybylski, M. *Phys. Rev. B* **2012**, *85*, 205417.

[11] Ünal, A. A.; Parabas, A.; Arora, A.; Ehrler, J.; Barton, C.; Valencia, S.; Bali, R.; Thomson, T.; Yildiz, F.; Kronast, F. *Ultramicroscopy* **2017**, *183*, 104-108.

[12] Yildiz, F.; Przybylski, M.; Ma, X. D.; Kirschner, J. *Phys. Rev. B* **2009**, *80*, 064415.

[13] Deger, C.; Ozdemir M.; Yildiz F. *J. Magn. Magn. Mater.* **2016**, *408*, 13-17.

[14] Rizal, C. *J. Magn. Magn. Mater.* **2007**, *310*, 646-648.

[15] Kehagias, T.; Komninou, P.; Christides, C.; Nouet, G.; Stavroyiannis, S.; Karakostas, T. *J. Cryst. Growth* **2000**, *208*, 401-408.

[16] Hrubovčák, P.; Zeleňáková, A.; Zeleňák, V.; Kováč, J. *J. Alloys Compd.* **2015**, *649*, 104-111.

[17] Yang, K.; Kryutyanskiy, V.; Kolmychek, I.; Murzina, T. V.; Lukaszew, A. R. *J. Nanomater.* **2016**, *87*, 1-7.

[18] Soohoo, R. *Phys. Rev.* **1960**, *120*, 1978-1982.

[19] Soohoo, R. *J. Appl. Phys.* **1961**, *32*, 148-150.

[20] Soohoo, R. *J. Appl. Phys.* **1981**, *52*, 2459-2461.

[21] Ozdemir, M. PhD, İstanbul Technical University, İstanbul, Turkey, 1998.

[22] Deger, C.; Aksu, P.; Yildiz, F. *IEEE T. Magn.* **2016**, *52*, 1-4.

[23] Christides, C. *Handbook of Surfaces and Interfaces of Materials*; Academic Press: San Diego, CA, USA, 2001.

[24] Verschoren, G.; Dobrynin, A. N.; Temst, K.; Silverans, R. E.; Van Haesendonck, C.; Lievens, P.; Pipeleers, B.; Zhou, S. Q.; Vantomme, A.; Bras, W. *Thin Solid Films* **2008**, *516*, 8232-8239.

[25] Rizal, C. L. S.; Yamada, A.; Hori, Y.; Ishida, S.; Matsuda, M.; Ueda, Y. *Phys. Status Solidi C* **2004**, *1*, 1756-1759.

[26] Pan, M. H.; Liu, H.; Wang, J. Z.; Jia, J. F.; Xue, Q. K.; Li, J. L.; Qin, S.; Mirsaidov, U. M.; Wang, X. R.; Markert, J. T. et al., *Nano Lett.* **2005**, *5*, 87-90.

[27] Bozorth, R. M. *Ferromagnetism*; Wiley: Hoboken, NJ, USA, 1993.

[28] Inoue, J. I.; Oguri, A.; Maekawa, S. *J. Phys. Soc. Jpn.* **1991**, *60*, 376-379.

[29] Emam, A. N.; Mansour, A. S.; Girgis, E.; Mohamed, M. B. In *Applying Nanotechnology for Environmental Sustainability*; Sung, H. J., Ed. IGI Global: Miami, FL, USA, 2016, pp. 231-275.